

Towards Mueller-Tang jets at Next-to-leading order

Federico Deganutti, Dimitri Colferai, Timothy Raben, Christophe Royon



DiffLow-x Meeting

Reggio Calabria

fedeganutti@ku.edu

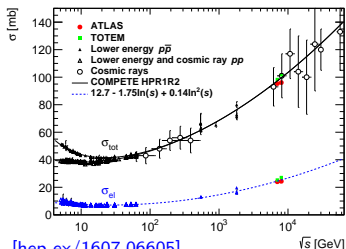
August 30, 2018

Outline

- Motivations and backgrounds
- Mueller-Tang jets at LL
- From LL to NLL
- Non-forward eigenfunction in momentum space
- NLO vet vertex
- Calculation strategy

Regge theory and the Pomeron

Regge Theory grew out of pre-QCD S-matrix theory of the 50's and 60's. Amplitudes are seen as unitary, Lorentz invariant functions of analytic momenta. (doesn't assume an underlying theory) At asymptotic energies $s \gg -t$, using partial wave analysis, the interaction is seen as an exchange of an *entire trajectory* of particles. The Pomeron is the dominant trajectory. $\sigma_{tot} \sim s^{\alpha_{\mathcal{P}}(t)-1}$ This soft Pomeron has been used to fit to p-p total cross sections since '70s.



Authors	$\alpha_{\mathcal{P}}(0)$
Donnachie-Landshoff (1992)	1.0808
Cudell, Kang and Kim (1997)	$1.096^{+0.012}_{-0.009}$
Cudell <i>et al.</i> (2000)	1.093 ± 0.003
COMPETE Collaboration (2002)	1.0959 ± 0.0021
Luna and Menon (2003)	1.085 - 1.104
Menon and Silva (2013)	1.0926 ± 0.0016

Promising tool to interpolate between perturbative and unperturbative regimes. What QCD has to say about the Pomeron?

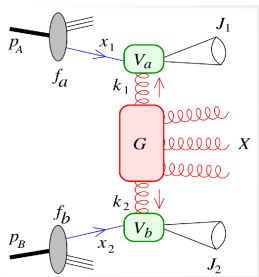
Looking at jets to see the Pomeron

Semi-hard regimes $s \gg -t \gg \Lambda_{QCD}$ QCDp \rightarrow BFKL resummation \rightarrow power-like growth of cross-section in s .

Mueller Navelet jets

$p + p \rightarrow jet_1 + jet_2 + anything\ else$ Tagged jets far apart in rapidity. Preferred testing ground for BFKL dynamics. Phenomenology study at NLL available [[arXiv:1010.0160](https://arxiv.org/abs/1010.0160)]

But.. at intermediate energies $\alpha_s \log(s/-t) < 1$ large contaminations from other limits (DGLAP, finite order) tend to hide the Pomeron signature. Need tuning of renorm. scale (BLM) and/or asymmetric observables (see [F. Celiberto Monday talk.](#))

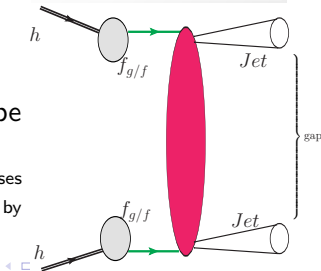


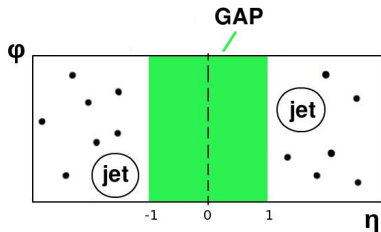
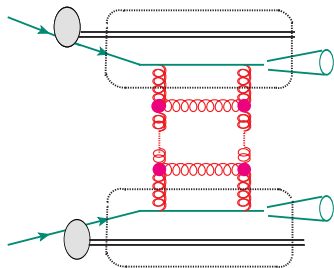
Mueller Tang jets

$p + p \rightarrow jet_1 + jet_2 + gap$

Dijets separated by a large rapidity gap can probe the finite-momentum structure of the Pomeron.

Subleading compared to M-N ($d\hat{\sigma} \propto \alpha_s^4$) but the lower background promises a cleaner recognition of the Pomeron contribution. cross-section lowered by proton remnant rescattering, I'll say few more words later...





- The absence of any additional emission over a large rapidity region suggests that the color-singlet exchange contributes substantially to the jet-gap-jet cross section.
- The BFKL predictions for these processes have been studied at LL accuracy and partially also at NLL order
- The last ingredients that have to be taken into account to complete the approximation order are the NLO impact factors

- Fixed rapidity gap $|\eta| < 1$, no charged particles *and* no photons or neutral hadrons with $p_T > 0.2 \text{ GeV}$.
- Dijet events with at least 2 hard jets with $p_T^{jet} > 40 \text{ GeV}$ and $|\eta^{jet}| > 1.5$

BFKL description of Mueller-Tang jets

BFKL dynamic effects

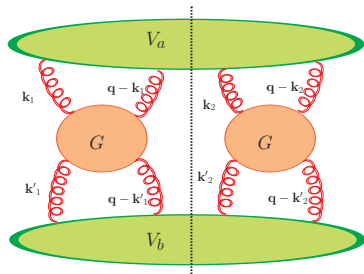
are predicted to appear as the rapidity Y between the two jets increases. The imposition of a veto on any other form of radiation favors the description of the interaction through the exchange of a color singlet compared to other color representations.

- In general the cross section for these processes is given as a multiple convolution between the the jet vertices and the GGFs.

$$\frac{d\hat{\sigma}}{dJ_1 dJ_2 d^2\mathbf{q}} = \int d^2\mathbf{k}_1 d^2\mathbf{k}'_1 d^2\mathbf{k}_2 d^2\mathbf{k}'_2 V_a(\mathbf{k}_1, \mathbf{k}_2, J_1, \mathbf{q}) \times \\ G(\mathbf{k}_1, \mathbf{k}'_1, \mathbf{q}, Y) G(\mathbf{k}_2, \mathbf{k}'_2, \mathbf{q}, Y) V_b(\mathbf{k}'_1, \mathbf{k}'_2, J_2, \mathbf{q}), \quad J = \{\mathbf{k}_J, x_J\}.$$

- The explicit form of the jet vertex and the Green function depends on the approximation level.

NLL vertex is known [[Hentschinski](#), [Madrigal Martinez](#), [Murdaca](#), [Sabio Vera](#)].



LL approximation: Non forward gluon Green function

The GGF is given by the Mellin transform of the function f_ω which is the solution of the BFKL equation. The solution of the non forward BFKL equation is more naturally expressed in the impact parameter space.

$$G(\mathbf{k}, \mathbf{k}', \mathbf{q}, Y) = \int_{-i \text{ inf}}^{+i \text{ inf}} \frac{d\omega}{2\pi i} e^{Y\omega} f_\omega(\mathbf{k}, \mathbf{k}', \mathbf{q})$$

$$f_\omega(\rho_1, \rho_2, \rho'_1, \rho'_2) = \frac{1}{(2\pi)^6} \sum_{n=-\text{inf}}^{+\text{inf}} \int_{-\text{inf}}^{+\text{inf}} d\nu \frac{R_{n\nu}}{\omega - \omega(n, \nu)} E_{n\nu}^*(\rho'_1, \rho'_2) E_{n\nu}(\rho_1, \rho_2)$$

$$E_{n\nu}(\rho_1, \rho_2) = \underbrace{\left(\frac{\rho_1 - \rho_2}{\rho_1 \rho_2} \right)^h \left(\frac{\rho_1^* - \rho_2^*}{\rho_1^* \rho_2^*} \right)^{\bar{h}}}_{\text{Lipatov term}} \underbrace{- \left(\frac{1}{\rho_2} \right)^h \left(\frac{1}{\rho_2^*} \right)^{\bar{h}} - \left(\frac{-1}{\rho_1} \right)^h \left(\frac{-1}{\rho_1^*} \right)^{\bar{h}}}_{\text{Mueller-Tang correction}}$$

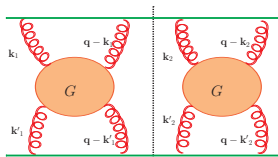
$E_{n\nu}$ are the eigenfunctions in the impact parameter space.

The GGF in momentum space is recovered applying a Fourier transformation to the eigenfunctions.

$$\tilde{E}_{n\nu}(\mathbf{k}, \mathbf{q}) = \int \frac{d^2 r_1 d^2 r_2}{(2\pi)^4} E_{n\nu}(\rho_1, \rho_2) e^{i(\mathbf{k} \cdot \mathbf{r}_1 + (\mathbf{q} - \mathbf{k}) \cdot \mathbf{r}_2)}$$

Pomeron exchange amplitude

With the leading order vertex independent from the loop momenta the partonic cross section can be expressed as the square modulus of an amplitude that is nothing more than the GGF integrated in its transverse momenta.



$$A(Y, q) = h_a^0 h_b^0 \int d^2 k d^2 k' G(\mathbf{k}, \mathbf{k}', q, Y), \quad \frac{d\hat{\sigma}}{dq dY} = \frac{1}{16\pi} |A(Y, q)|^2$$

The amplitude can be written in terms of the averaged eigenfunctions

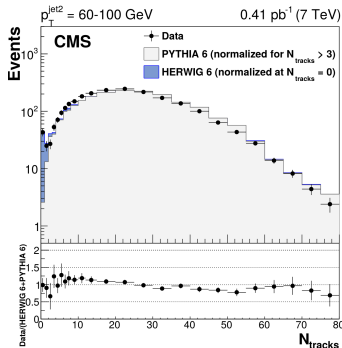
$$\bar{E}_{n\nu}(\mathbf{q}) = \int d^2 k \bar{E}_{n\nu}(\mathbf{k}, \mathbf{q}).$$

The integration over the transverse momenta greatly simplifies the calculation of the Fourier transform of the eigenfunctions canceling the Lipatov term contribution. The Pomeron exchange amplitude is given by the simple expression

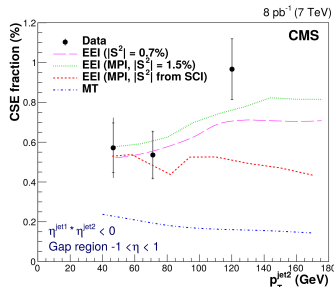
$$A(Y, q) = h_a^0 h_b^0 \sum_{n=-\text{inf}}^{+\text{inf}} \int_{-\text{inf}}^{+\text{inf}} d\nu e^{Y\omega_{n\nu}} R_{n\nu} \left(\frac{4}{\mathbf{q}^2} \right)$$

This can be easily extended to include the GGF at NLL $\omega^{LL}(n, \nu) \rightarrow \omega^{NLL}(n, \nu)$.

Previous fits and analysis



- Charged-particle multiplicity in the gap region between the tagged jets compared to PYTHIA and HERWIG predictions.
- HERWIG 6: include contributions from color singlet exchange (CSE), based on **BFKL at LL**.
- PYTHIA 6: inclusive dijets (tune Z2*), **no-CSE**.

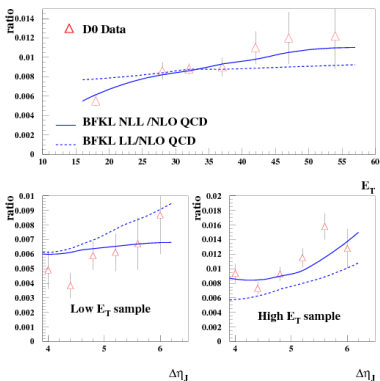


$$f_{CSE} = \frac{N_{\text{events}}^F - N_{\text{non-CSE}}^F}{N_{\text{events}}}$$

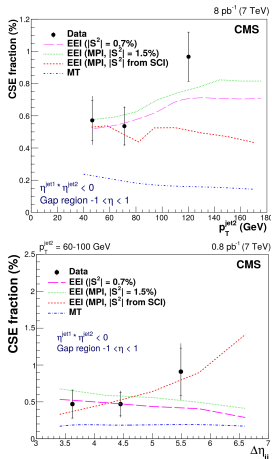
A closer look shows the failure of the MT model in reproducing any detail of the observed distribution. Not surprising considering the size of the NLL corrections.

[CMS-PAS-FSQ-12-001]

Previous fits and analysis



- Ratio $R = \frac{NLL * BFKL}{NLO QCD}$ of jet-gap-jet events to inclusive dijet events as a function of p_T and the rapidity gap Y .

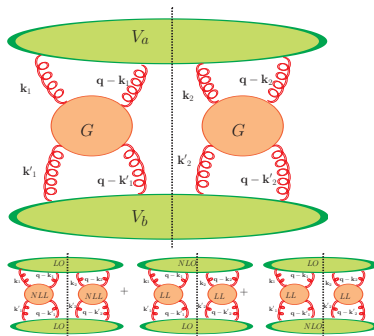


NLL* BFKL calculations different implementations of the soft rescattering processes (EEI models), describe many features of the data, but none of the implementations is able to simultaneously describe all the features of the measurement. Ekstedt, Enberg, Ingelman, [1703.10919]

incorporating NLO jet vertex

A full NLL/O calculation is within reach.
 NLO MT impact factors recently calculated.
 Very complicated! (not in a factorizable form!)

But...only certain combinations of jet vertex and Green's function approximation orders contribute effectively to the NL order of the cross section.

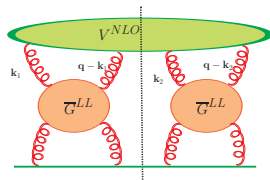


- GGF NLL + LO vertices. Simplest case. Cross section as amplitude squared.
- GGF LL + LO vertex + NLO vertex. The non trivial dependence of the NLO jet vertex from the reggeon momenta introduces an important complication.
- GGF LL + both NLO vertices. Discarded because subleading.

The decision to keep just the pure NL contribution brings some simplification

$$\frac{d\hat{\sigma}}{dJ_1 dJ_2 d^2\mathbf{q}} = \int d^2k_1 d^2k_2 V^1(\mathbf{k}_1, \mathbf{k}_2, \mathbf{q}; J_1) \times$$

$$\underbrace{\int d^2k'_1 G(\mathbf{k}_1, \mathbf{k}'_1, \mathbf{q}, Y)}_{\bar{G}(\mathbf{k}_1, \mathbf{q}, Y)} \underbrace{\int d^2k'_2 G(\mathbf{k}_2, \mathbf{k}'_2, \mathbf{q}, Y)}_{\bar{G}(\mathbf{k}_2, \mathbf{q}, Y)} V^0(J_2, \mathbf{q})$$



- Large increase in computation time due to the high-dimensional multiple integration.

The average \bar{G} is

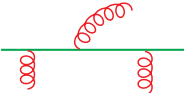
$$\bar{G}(x_1 x_2, q, \Delta\theta, k) = \tilde{E}_{n\nu}(\mathbf{k}, \mathbf{q} - \mathbf{k}) \int dk'^2 \tilde{E}_{n\nu}(\mathbf{k}', \mathbf{q} - \mathbf{k}') = \tilde{E}_{n\nu}(\mathbf{k}, \mathbf{q} - \mathbf{k}) \bar{E}_{n\nu}^*(q).$$

The full form of the eigenfunction in momentum space $\tilde{E}_{n\nu}(k, k')$ is known [Bartels, Braun, Colferai, Vacca] but it has been proven very hard to implement.

- The momentum dependence of the eigenfunction is expressed through Gauss hypergeometric functions.

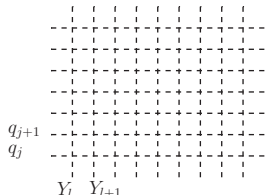
Numerical analysis

Peculiar characteristics of the NLO the jet vertex.

- Non trivial dependence from the reggeon momenta \rightarrow “connects” the two GGFs over the cut. 
- Up to two partons emitted by the same vertex \rightarrow dependence from the jet reconstruction algorithm. (1) The two partons form the same jet or (2) one of the two has energy lower than the calorimeter threshold and so it is not detected.
- The parton emission below threshold in the prohibited region alter the alignment between the forward and the backward jet. Jets not back-to-back anymore $\hat{\sigma}(q, Y) \rightarrow \hat{\sigma}(k_{J_1}, k_{J_2}, \theta_{J_2, J_2}, Y)$.
- Calculation of the partonic cross section.

(1) \bar{G} as a grid of its parameters $\{k_i, q_j, \theta_l, Y_m\}$. It involves a numerical integration over ν and a sum over n for each set of the parameters.

(2) Partonic cross section as the interpolation of \bar{G} grids and the NLO vertex.



$$\frac{\hat{\sigma}(k_{J_1}, k_{J_2}, \theta_{J_1, J_2}, Y)}{dk_j dY} \propto \sum V(k_{1_i}, k_{2_j}, \theta_{1_n}, \theta_{2_m}, J) \bar{G}(k_{1_i}, q_r, \theta_{1_n}, Y_l) \bar{G}(k_{2_j}, q_r, \theta_{2_m}, Y_l)$$

Numerical analysis

The non-forward BFKL eigenfunction at LL is given in terms of Gauss hypergeometric functions.

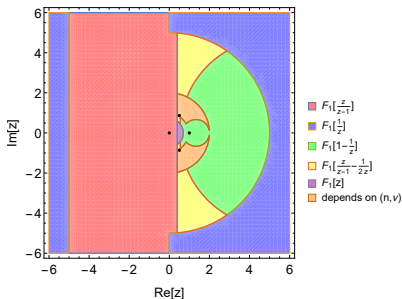
$$\tilde{E}_{n\nu}(k, k') \propto \left[k^{*\bar{h}-2} k'^{*h-2} {}_2F_1\left(1-h, 2-h; 2, -\frac{k}{k'}\right) {}_2F_1\left(1-\bar{h}, 2-\bar{h}; 2, -\frac{k'}{k_1^*}\right) + \{1 \rightarrow 2\} \right]$$

$$k' = q - k, \quad h = \left(\frac{1+n}{2} + i\nu\right), \quad \bar{h} = \left(\frac{1-n}{2} + i\nu\right)$$

Hypergeometric functions are hard to compute. ${}_2F_1(a, b; c, z) = \sum_n \frac{(a)_n (b)_n}{(c)_n} \frac{z^n}{n!}$
 What about the rest of the complex plane?

Several transformations connect the various regions of the complex plane: $z, \frac{1}{z}, \frac{1}{z-z_0}, \frac{z-1}{z}$. Special care must be taken for $b-a \simeq \mathbb{Z}^-$ and near $z = \{0, 1, \text{inf}, \exp(\pm i\pi/3)\}$.

Michel and Stoitsov [arXiv:0708.0116, math-ph], Doornik, [Math. Comp. 84 (2015), 1813-1833].



Numerical analysis

None of the cited codes for the hypergeometric function work for $\Im(a), \Im(b) \gtrsim 7$.

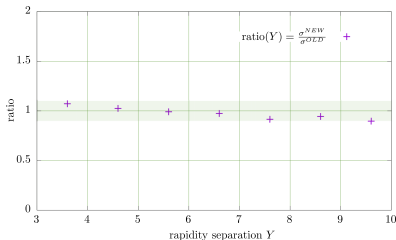
$$\bar{G}(x_1 x_2, q, \Delta\theta, \frac{k}{k'}) \propto \sum_m^{\text{even}} \int d\nu [k^{*\bar{h}-2} k'^{h-2} {}_2F_1\left(1-h, 2-h, 2; -\frac{k}{k'}\right) {}_2F_1\left(1-\bar{h}, 2-\bar{h}, 2; -\frac{k'^*}{k^*}\right) + \{1 \leftrightarrow 2\}].$$

- Integrand is highly oscillatory and slowly falling with ν . Need to integrate up to very large values of ν ($\gtrsim 100$). $h = \frac{1+n}{2} + i\nu$
- Bending the contour helps but for some z the two terms rise with ν and convergence is met only after the sum is taken.

Solution: Patch different methods depending on the parameters.

- (1) Summing the series.
 - (2) integrating the differential equation.
 - (3) Steepest descent estimate of the asymptotic expansion for large ν .
- Check the code against the known pure LL contribution to MT

$$\text{ratio}(q, Y) = \frac{\bar{G} \otimes \bar{G}^*}{|A(q, Y)|^2}$$



Outcomes

What has been done..

- Implementation of Gauss hypergeometric function is finally general enough to be used for the non-forward BFKL eigenfunction.
- Code up and running for generation of gluon-Green function grids to interpolate with the NLL impact factors.

What's next..

- Run code on HPC at KU (40 cores at 2.4 GHz with 192 GB 2666 MHz DDR4 memory) .
- Look at the NLL vertex corrections and play with the observable definition to identify physical region where cross-section is “more factorizable” .
- Include full corrections into MC generator with *ad hoc* parametrization.
- Where else can be useful the momentum space BFKL eigenfunction?

Details of NLO jet vertex

$$\begin{aligned}
 & \frac{d\hat{V}^{(1)}(x, \mathbf{k}, l_1, l_2; x_J, \mathbf{k}_J; M_{X,\max}, s_0)}{dJ} = \\
 & = v_q^{(0)} \frac{\alpha_s}{2\pi} \left[S_J^{(2)}(\mathbf{k}, x) \cdot \left[-\frac{\beta_0}{4} \left[\left\{ \ln \left(\frac{l_1^2}{\mu^2} \right) + \ln \left(\frac{(l_1 - \mathbf{k})^2}{\mu^2} \right) + \{1 \leftrightarrow 2\} \right\} - \frac{20}{3} \right] - 8C_f \right. \right. \\
 & + \frac{C_a}{2} \left[\left\{ \frac{3}{2k^2} \left[l_1^2 \ln \left(\frac{(l_1 - \mathbf{k})^2}{l_1^2} \right) + (l_1 - \mathbf{k})^2 \ln \left(\frac{l_1^2}{(l_1 - \mathbf{k})^2} \right) - 4|l_1||l_1 - \mathbf{k}| \phi_1 \sin \phi_1 \right\} \right. \right. \\
 & \left. \left. - \frac{3}{2} \left[\ln \left(\frac{l_1^2}{k^2} \right) + \ln \left(\frac{(l_1 - \mathbf{k})^2}{k^2} \right) \right] - \ln \left(\frac{l_1^2}{k^2} \right) \ln \left(\frac{(l_1 - \mathbf{k})^2}{s_0} \right) - \ln \left(\frac{(l_1 - \mathbf{k})^2}{k^2} \right) \ln \left(\frac{l_1^2}{s_0} \right) - 2\phi_1^2 + \{1 \leftrightarrow 2\} \right\} + 2\pi^2 + \frac{14}{3} \right] \\
 & + \int_0^1 dz \left\{ \ln \frac{\lambda^2}{\mu_F^2} S_J^{(2)}(\mathbf{k}, zx) \left[P_{qq}(z) + \frac{C_a^2}{C_f^2} P_{gq}(z) \right] + \left[(1-z) \left[1 - \frac{2}{z} \frac{C_a^2}{C_f^2} \right] + 2(1+z^2) \left(\frac{\ln(1-z)}{1-z} \right)_+ \right] S_J^{(2)}(\mathbf{k}, zx) + 4S_J^{(2)}(\mathbf{k}, x) \right\} \\
 & + \int_0^1 dz \int \frac{d^2 \mathbf{q}}{\pi} \left[P_{qq}(z) \Theta \left(\hat{M}_{X,\max}^2 - \frac{(\mathbf{p} - z\mathbf{k})^2}{z(1-z)} \right) \Theta \left(\frac{|\mathbf{q}|}{1-z} - \lambda \right) \right. \\
 & \quad \times \frac{k^2}{q^2(\mathbf{p} - z\mathbf{k})^2} S_J^{(3)}(\mathbf{p}, \mathbf{q}, (1-z)x, x) + \Theta \left(\hat{M}_{X,\max}^2 - \frac{\Delta^2}{z(1-z)} \right) S_J^{(3)}(\mathbf{p}, \mathbf{q}, zx, x) P_{gq}(z) \\
 & \left. \times \left\{ \frac{C_a}{C_f} [J_1(\mathbf{q}, \mathbf{k}, l_1, z) + J_1(\mathbf{q}, \mathbf{k}, l_2, z)] + \frac{C_a^2}{C_f^2} J_2(\mathbf{q}, \mathbf{k}, l_1, l_2) \Theta(\mathbf{p}^2 - \lambda^2) \right\} \right] \left. \right]
 \end{aligned}$$

$$\tilde{E}_{n\nu}(k_1, k_2) =$$

$$N(n, \nu) \left[k_1^{*\bar{h}-2} k_2^{*h-2} {}_2F_1(1-h, 2-h; 2, -\frac{k_1}{k_2}) {}_2F_1(1-\bar{h}, 2-\bar{h}; 2, -\frac{k_2^{**}}{k_1}) + \{1 \rightarrow 2\} \right]$$

$$h = \left(\frac{n+1}{2} + i\nu\right), \quad \bar{h} = \left(\frac{n-1}{2} - i\nu\right)$$

∈

for example for $|z| > 1$ and $d = b - a$:

$${}_2F_1(a, b; c, z) = \frac{\Gamma(c)\Gamma(-d)}{\Gamma(a)\Gamma(c-b)} (-z)^{-b} {}_2F_1(b, 1-c+b; 1+d, \frac{1}{z}) + \{a \rightarrow b\}$$

each term naively diverges when dZ